Comparison Between Serial and Parallel Concatenated Channel Coding Schemes Using Continuous Phase Modulation over AWGN and Fading Channels

Manjeet Singh (ms308@eng.cam.ac.uk) - presenter
Ian J. Wassell (ijw24@eng.cam.ac.uk)

Laboratory for Communications Engineering
Department of Engineering
University of Cambridge
Fax: 0044-1223-766517 Tel: 0044-1223-765150

Abstract

A generic M-ary continuous phase modulation (CPM) scheme, with a modulation index of $h = 1/M$, can be decomposed into a continuous-phase encoder (CPE) followed by a memoryless modulator (MM), where the CPE is linear over the ring of integers modulo M (M being the code radix). Thus, for a binary CPM scheme, M = 2 while for a quaternary scheme, M = 4. By designing a channel encoder (CE), which is a convolutional encoder, to operate over the same ring of integers modulo M, the CE and the CPE can be combined to create another M-ary convolutional encoder called an extended CE. In this paper, we use a code radix of 4 i.e. M = 4. Here, a ½ rate CE over the ring of integers modulo 4 is combined with the CPE of a 4-ary CPM scheme whose modulation index is h = ¼ to create a quaternary extended CE. Using this trellis coded modulation design, the paper compares the performance of a serial and a parallel-concatenated channel-coding scheme over AWGN and Rayleigh slow flat fading channels. In both schemes, the inner encoder is the quaternary extended CE and the outer encoder is another quaternary convolutional encoder. Due to its lower code rate, the parallel scheme has a better BER performance than the serial scheme. The coding gain is, however, modest. For the parallel scheme, a BER of 2.8 X 10^{-4} was attainable at 4 dB E_b/N_0 in the AWGN channel.

Keywords: Concatenated channel coding, Continuous Phase Modulation, Convolutional, Decomposed Model, Parallel, Serial.

1. Introduction

Since the pioneering work of Ungerboeck in 1982, trellis-coded modulation (TCM) has become an effective coding technique for bandlimited channels. By using TCM with memoryless modulations, such as *M*-ary phase shift keying (MPSK) or quadrature amplitude modulation (QAM), significant coding gains can be achieved without bandwidth expansion. Studies have also been done that combine encoders with memory modulation schemes [1]. One such modulation scheme is continuous phase modulation (CPM).

CPM is a form of constant-envelope digital modulation and therefore of interest for use with nonlinear and/ or fading channels. The inherent bandwidth- and energy efficiency makes CPM a very attractive modulation scheme. Furthermore, CPM signals have good spectral properties due to their phase continuity.

Besides providing spectral economy, CPM schemes exhibit a “coding gain” when compared to PSK modulation. This “coding gain” is due to the memory that is introduced by the phase-shaping filter and the decoder can exploit this. CPM modulation exhibits memory that resembles in many ways how a convolutionally encoded data sequence exhibits memory - in both cases, a “trellis” can be used to display the possible output signals (this is why convolutional encoders are used with CPM in this paper).

Massey in [2] suggested that CPM could be decomposed into two parts: a continuous

phase encoder (CPE) with memory, and a memoryless modulator (MM). Such decomposition has two advantages [4]. Firstly, the "encoding" operation can be studied independently of the modulation. The second advantage is that the isolation of the MM would allow the cascade of the MM, the waveform channel (e.g. additive white Gaussian noise (AWGN)) and the demodulator to be modeled as a discrete memoryless channel.

In [3, 4, 5], Rimoldi derived a generic decomposition model of an *M*-level CPFSK (*M* being the code radix), comprising a CPE and an MM. He showed that the CPE is a linear (modulo some integer *M*) time-invariant encoder and the MM another time-invariant device. It is then of interest to optimally combine a convolutional coder with the CPE to create a trellis coded modulation scheme.

Li in [6] has given a list of some convolutional encoders that can be combined with the CPE without the use of a mapper. To facilitate this, both the encoder and the CPE must operate over the same algebra structure. This is unlike the usual approach where mappers are pertinent [1, 7].

In this paper, we combine a quaternary ($M = 4$) convolutional encoder, hereafter called a *channel encoder* (CE), with the CPE of a quaternary CPM scheme. Such a combination is called an extended CE and is effectively a quaternary convolutional encoder. We compare the performance between a serial and a parallel-concatenated channel-coding scheme. In both schemes, the outer encoder is a ½ rate convolutional encoder operating over the ring of integers modulo 4 while the inner encoder is a ½ rate quaternary extended CE. A code rate of ½ implies that for each input bit entering the encoder, it outputs two bits. The CPM scheme employs a 2 raised cosine (2*RC)* filter and has a modulation index of $h = ¼$. Only hard decision decoding (HDD) techniques are investigated. HDD implies that the decoder only provides the decoded data sequence, without providing any measure of how reliable the decoding sequence was. Providing reliable information is the realm of soft decision decoding (SDD), which is not investigated here. Decoding is based on the Viterbi algorithm, which is a maximum likelihood sequence estimator. Simulations are executed over an AWGN channel and a Rayleigh slow flat fading channel. The use of interleavers between the inner and outer encoder, is also investigated.

2. System Design

The section explains the design of the two channel coding schemes considered in the study. The serial concatenated channel-coding (SCCC) scheme is shown in Figure 1. It has an outer ½ rate quaternary convolutional encoder while the inner encoder is the ½ rate quaternary extended CE. As both the inner and outer encoders operate over the same algebra structure, no mapper is required to concatenate them.

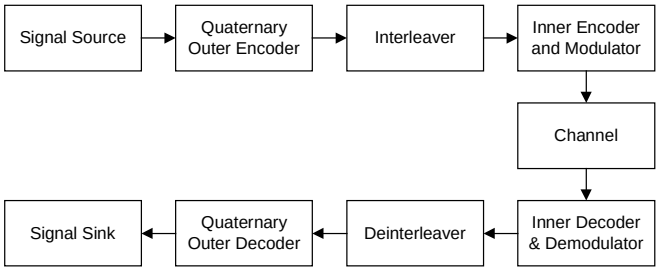

Figure 1. Generic set up of the serially concatenated coding system.

The parallel-concatenated channel-coding (PCCC) scheme is shown in Figure 2. It has 2 ½ rate outer quaternary encoders connected in parallel by a 5 x 5 block interleaver. The outputs from these encoders are multiplexed by a commutator switch and fed to the inner encoder. In both the SCCC and PCCC schemes, the inner and outer quaternary decoders perform HDD.

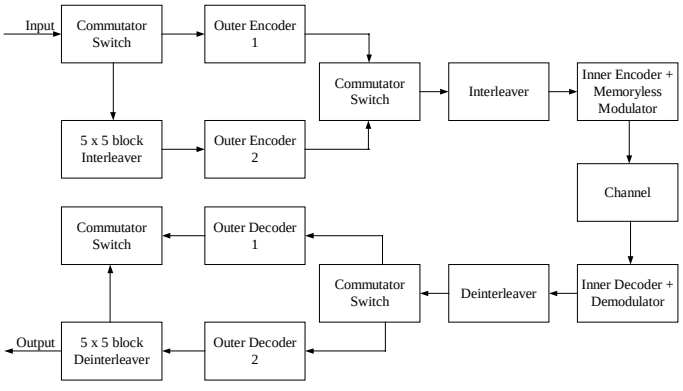

Figure 2. Generic set up of the parallel concatenated coding system.

2.1. Design of the extended CE

Figure 3 shows the design of the extended CE, which is the inner encoder for both the SCCC and PCCC schemes. For the purpose of system evaluation, a 2*RC* (partial-response) scheme with $h = ¼$ ($M = 4$) was implemented using the baseband decomposed CPM model. The CPE has two memory (delay) cells. One cell stores the previous transmitted symbol while the other memory cell stores the sum (mod 4) of all previously transmitted symbols. As the phase response of the incoming signal lasts two symbol intervals (L=2), controlled intersymbol interference is introduced.

The extended CE is a ½ rate quaternary convolutional encoder. It has 3 memory cells (memory cells D1 and D2 form part of the CPE) and generates 64 states (4^3). As there are 4 branches/ waveforms emanating from and arriving at each state and each "analog" waveform is made of 8 samples, a total of 8 X 4 X 64 = 2048 waveform samples would require processing for the extended CE at each iteration of the Viterbi algorithm.

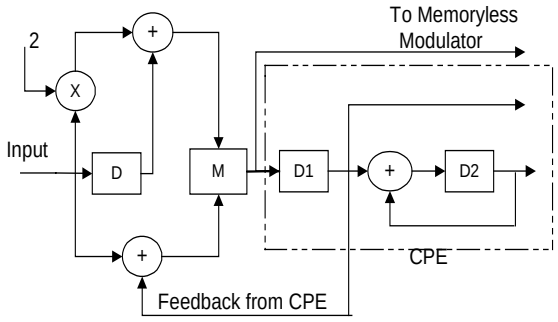

Figure 3. ½ rate extended CE with feedback from the CPE. D denotes a memory cell while M denotes a multiplexer. Additions are all modulo 4. D1 and D2 are the memory cells of the CPE.

By designing the CE to operate over the same algebra as the CPE, no mapper is required to integrate them. This allows the state of the CPE to be fed back and be used by the CE enabling the use of a CE with a shorter constraint length. Such a combination is called an extended CE, as the CPE is now an extension of the CE.

2.2. Design of the Memoryless Modulator

The memoryless modulator contains a raised cosine (*RC*) phase shaping function which is implemented by two finite impulse response (FIR) digital filters, FIR filter A and FIR filter B as shown in Figure 4 above. In this study, each output waveform is made up of eight discrete samples.

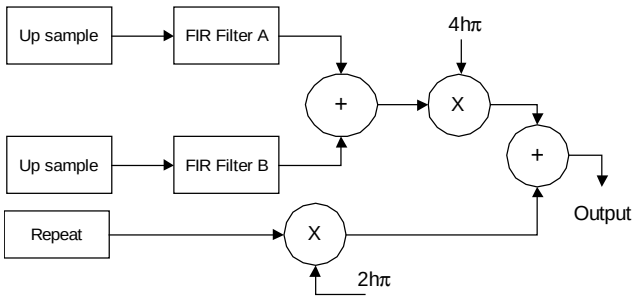

Figure 4. Block diagram of the memoryless modulator. The Up Sample and Repeat blocks increase the samples of the input signals by a factor of 8. h denotes the modulation index.

2.3. Design of the Outer Encoders

The design of the outer quaternary convolutional encoder is shown in Figure 5. It has a constraint length of 3 and a generator polynomial of $(6, 17)_{10}$. It also operates over the ring of integers modulo 4, similar to the extended CE.

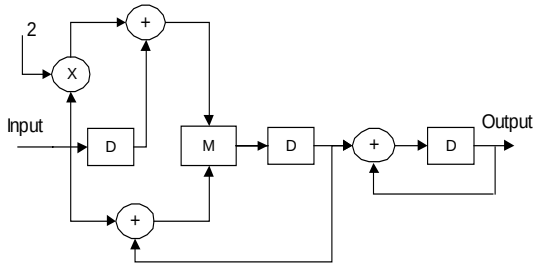

Figure 5. ½ rate quaternary outer encoder. The design is quite similar to the extended CE. Additions are all modulo 4. D and M denote the memory cells and multiplexer respectively.

2.4. Design of the Hard Viterbi Decoders

A general overview of the Viterbi hard decision decoder is shown in Figure 6. Both the inner and outer decoders have the same design.

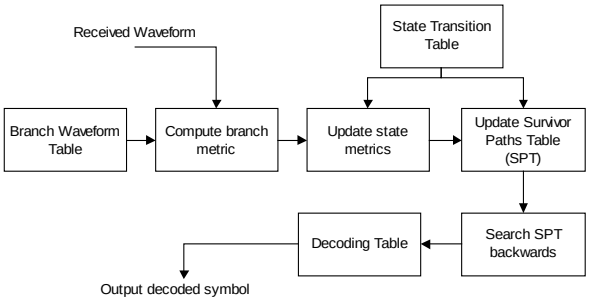

Figure 6. High-level diagram of the Viterbi Decoders

Decoding is based on a technique called *list decoding*. This technique entails storing all the possible waveforms the encoder can generate as a list in a random-access-memory (RAM) at the front end of the decoder. When a waveform is received, (corrupted by additive noise or fading), the Euclidean distances between it and all the possible waveforms in the list are calculated. These distances (or branch metrics) serve as a probability that a given waveform/ symbol was actually sent. The smaller the Euclidean distance, the higher the probability that a specific waveform was sent. However, these branch metrics are not used in isolation. They are used in conjunction with the probabilities (state metrics) associated with the states of the trellis that each of the branches departs from. In this way, the Euclidean distance between the entire received sequence and the most likely path through the trellis can be calculated on a symbol-by-symbol basis.

The decoders make use of three tables to facilitate demodulation/decoding of the received waveform. These tables are generated by the encoder/modulator and stored in RAMs in the decoder. For the outer decoder, only the outer encoder was used to generate the tables. For the inner decoder, the inner encoder and the memoryless modulator generate the tables. The three tables are:

a. State Transition Table - which takes as its inputs the current state and input symbol and outputs the next state.

b. Waveform Table – which takes as inputs the current state and symbol input and generates the output waveform. This table contains the list of all the possible waveforms that can be generated by the encoders. This is the first table used in the decoding/demodulation process.

c. Decoding Table – which takes as its inputs the current state and previous state and outputs the transmitted symbol.

It is assumed that there are no parallel transitions between states. The advantage of using these tables is that for the same value of L the Viterbi decoders need not be redesigned for each new scheme to accommodate more or less states or a different symbol alphabet size.

3. Methodology

The research methodologies involve detailed computer simulations of the communication systems under consideration. The simulations were performed using the Cadence Signal Processing Workstation (SPW) Version 4.1 running on a dual processor SPARC 10 workstation. The results of the computer simulations are displayed using graphs in which the bit error rates (BER) are plotted against E_b/N_o (energy-per-bit to noise density ratio). To facilitate proper comparison between the two coding schemes, E_b/N_o is used rather than SNR (signal to noise ratio). This is because of the difference in code rates of the two schemes. The SCCC scheme has an overall code rate of ¼ while the PCCC scheme has a code rate of $\frac{1}{8}$.

The method of determining the BER in this research is shown in Figure 7. The processed signal, after the receiver is compared with the signal generated by the random generator. Any bit difference between the two signals constitutes a bit error and is accumulated and recorded in the BER counter.

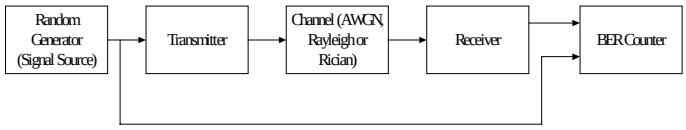

Figure 7. Method to determine BER

Almost all radio communications systems occupy a relatively narrow bandwidth, B, centered on the carrier frequency f_c, where $f_c >> B$. These are known as bandpass systems. Bandpass signals are the result of using narrow bandwidth baseband signals (centered around 0Hz) to modulate a relatively high frequency sinusoidal signal (called the carrier). The result is a frequency translation of the baseband signal, making the original information more suitable for transmission through the channel. This is

essential for physical transmissions, however, for simulation purposes, it will result in an excessively high number of samples per second. To reduce the sampling rate and to simplify system analysis, an equivalent complex baseband (low pass) model of the actual modulated (or bandpass) system is adopted here. These baseband signals are, in general, complex and centered around 0 Hz and occupy the same basewidth *B* as before. Details of this technique are found in [8].

4. Channel Models Used

It is very important for simulations to implement adequate channel models describing real scenarios, for example satellite-to-earth stations, ship-to-home port, mobile station-to-base station, a telephone line between modems and so on. Both the modulator and encoder should be designed so that system requirements are satisfied as efficiently as possible. One should use channel models that accurately describe the channel distortion. This allows one to implement different modulation and coding techniques and choose the best one based on system requirements.

Here, the simulations are simulated over two types of channels. The first is the additive white Gaussian noise (AWGN). This is an example of a *memoryless* channel. In such channels, the present are not influenced by the past. The other channel considered is the Rayleigh slow flat fading channel. This is a channel with memory.

4.1. AWGN Channel Model

The Gaussian channel is important for providing an upper bound on system performance. For a given modulation scheme, the BER performance in AWGN can be calculated or measured in the laboratory. When multipath fading occurs, the BER will increase for a given channel SNR. By using techniques to combat multipath fading, such as diversity, equalization, data interleaving, and so on, it can be observed how close the BER approaches that for the Gaussian channel, in other words, the channel offers a kind of datum.

The Gaussian channel used here is shown in Figure 8. Based on the input signal, and the bandwidth of the noise, the noise is generated and added to the signal. This signal is then input to the demodulator/ decoder to be processed.

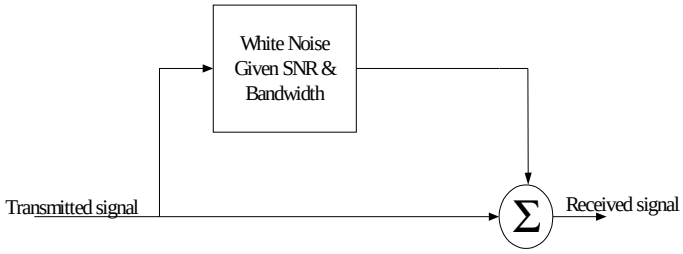

Figure 8. Gaussian noise model

4.2. Rayleigh Slow Fading Channel Model

The arrangement of the Rayleigh slow, flat fading channel is illustrated in Figure 9. As we have assumed a very slow fading channel, any phase shifts in the received signal can be corrected. The phase correction circuitry is shown enclosed by a doted ellipse. Its function is to remove the phase shift caused by the Rayleigh flat fading (RFF) block by subtracting it (via complex exponential multiplication) from the received signal. This process, actually, corresponds with ideal coherent demodulation.

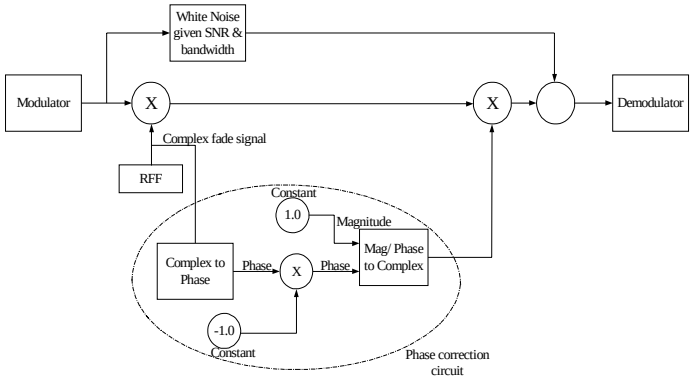

Figure 9. Model of Rayleigh slow, flat fading channel, showing phase correction blocks

5. Simulations and Results

The entire coding system was built in software and tested using Monte Carlo based simulations. The results obtained are in terms of the bit error rate (BER) as a function of the bit energy to noise density ratio (E_b/N_0). In all the simulations, a normalized bandwidth of BT_s = 1.2 was assumed where B is the bandwidth and T_s the symbol duration. For the quaternary 2*RC* scheme, this bandwidth contains approximately 99.97% of the total power.

For the SCCC system, the overall code rate was ¼ (both the inner and outer encoders

have a code rate of ½). This meant that for each input symbol to the encoder, four symbols were output to the modulator. The overall code rate of the PCCC system was $\frac{1}{8}$ (the parallel outer encoders had an overall code rate of ¼ while the inner encoder had a code rate of ½). For both concatenated coding schemes, the inner and outer encoders each have 64 states.

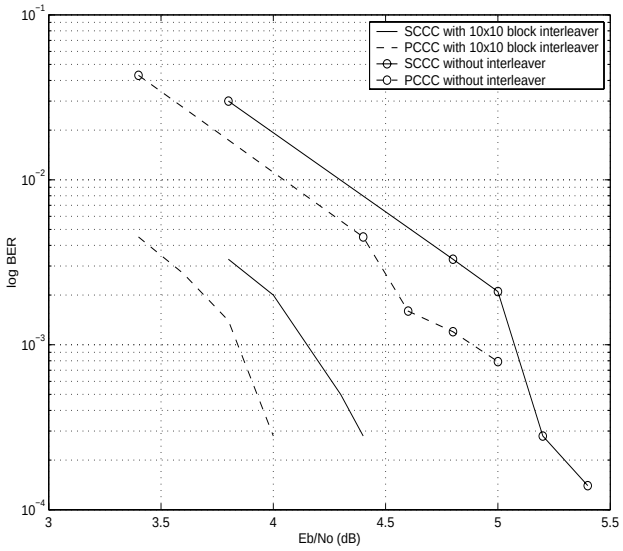

Figure 10. BER performance with and without a 10 x 10 block interleaver over an AWGN channel.

Figure 10 shows the BER performance of the coding schemes simulated over an AWGN channel, with and without the use of interleavers between the outer and inner encoders. Figure 11 shows the BER performance over the Rayleigh slow flat fading channel with a 10 x 10 block interleaver. In both channels, the BER performance of PCCC schemes was modestly better than the SCCC schemes. This is due to the higher code rate of the PCCC scheme. In terms of the coding gain:

- In the AWGN channel, a gain of 0.2dB was attained at a BER of 10^{-3} without the interleaver. With a 10 x 10 block interleaver, the gain was 0.4dB at a BER of 3×10^{-4}.
- In the Rayleigh channel, a gain of 0.1dB was attained at a BER of 10^{-3}.

The coding gains seem to be quite modest. The receiver in the PCCC scheme requires more synchronized circuits to synchronize the two parallel paths. For both schemes, the speed of processing the data was about the same. However, both schemes do provide very good BER performances. For example, at 4dB E_b/N_0, a BER of 2.8×10^{-4} was attained in an AWGN channel with the PCCC scheme. At 4.4dB E_b/N_0 the same BER can be attained with the SCCC scheme.

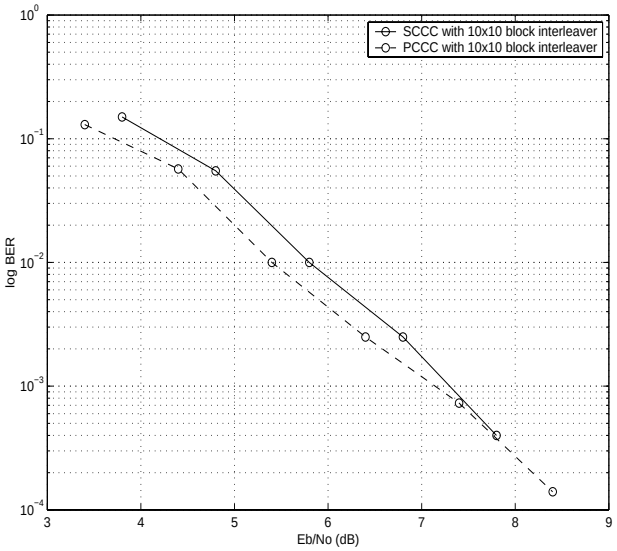

Figure 11. BER performance with a 10 x 10 block interleaver over Rayleigh fading channel.

6. Discussions and Conclusion

Previous works [3, 5] have suggested decomposing a CPM modulator and combining the CPE with a CE naturally i.e. without a mapper. To enable this, both the CE and the CPE must operate over the same algebra structure. In this paper, we designed a serial and a parallel-concatenated channel coding scheme and tested them both in an AWGN and a Rayleigh slow flat fading channel.

Due to its lower code rate, The BER performance of the PCCC scheme was slightly better than the SCCC scheme. The coding gains attained were, however, quite modest when considering the complexity of the receiver in the PCCC scheme. The receiver requires two outer decoders and more synchronization circuits to synchronize the two parallel paths. Speed in processing the received signals was found to be the same in both schemes. Both schemes do provide very good BER, comparable to some turbo designs that use large interleavers and employ a large number of iterations. The potential areas of application of such coding schemes are in the improvement of already established standards, for example GSM and cellular digital packet data and for speech

transmissions, where a BER of 10^{-3} is quite acceptable.

7. Acknowledgements

The authors would like to thank the Laboratory for Communications Engineering (Cambridge University) for the use of their equipment in the research and the Center for Wireless Communications (National University of Singapore) for their assistance.

8. References

[1] J.B. Anderson, T. Aulin and C.E. Sundberg, "Digital Phase Modulation", New York: Plenum, 1986.

[2] J.L Massey, "*The how and why of channel coding*," in Proc. Int. Zurich Seminar, Mar.1984, pp. F11(67)-F17(73).

[3] B. Rimoldi, "*A decomposed approach to CPM*," IEEE Trans. Inform. Theory, vol.34, pp.260-270, Mar.1988.

[4] B. Rimoldi, "*Continuous phase modulation and coding from bandwidth and energy efficiency*," PhD dissertation, Swiss Fed. Inst. Technol., 1988.

[5] B. Rimoldi, "*Design of coded CPFSK modulation system for bandwidth and energy efficiency*," IEEE Trans.Commun., vol.37, pp. 897-905, Sept.1989.

[6] Quinn Li, "*On bandwidth and energy efficient digital modulation schemes*," PhD dissertation, Sever Institute, University of Washington, 1996.

[7] S.V. Pizzi and S.G. Wilson, "*Convolutional coding combined with Continuous Phase Modulation*," IEEE Trans. Commun., vol.33, pp.20-29, Jan.1985.

[8] J. G. Proakis and M. Salehi, "*Communication Systems Engineering*", Prentice Hall Inc, New Jersey, 1994.

Name of Conference: **CIC' 2001**

Paper ID : **CIC-singh-010**